

Flare Loop Geometry

Nariaki NITTA

*Lockheed Martin Solar and Astrophysics Laboratory
O/H1-12, B/252, 3251 Hanover Street, Palo Alto, CA 94304, U. S. A.
E-mail: nitta@lmsal.com*

Abstract

We discuss how much we can learn about the geometry of flare loops from the X-ray imagery presently available. The stereoscopic techniques, which make use of different projections caused by solar rotation, are not applicable to flare loops, because of their dynamic nature. With an assumption that the loop is contained in a plane, a single image provides a family of loop shapes as a function of the inclination angle of the loop plane with respect to the plane normal to the surface. It appears that various ways exist that may enable us to constrain the inclination angle.

Key words: Sun: corona — Sun: flares — Sun: X-rays,gamma-rays

1. Introduction

In recent years, there has been a growing recognition of the importance of magnetic reconnection in various solar settings, notably flares, (e.g., Tsuneta 1996), largely on the basis of high-resolution X-ray images from the *Yohkoh* spacecraft (Ogawara et al. 1991). Specifically, the signatures predicted in reconnection models are seen most strikingly in images of limb flares. This means that our understanding of how reconnection works is basically restricted to 2-d topology. A natural extension to the achievements so far made is to characterize flare loops in 3-d, preferably in disk events.

In order to retrieve the information on the dimension perpendicular to the plane of sky, measurements of Doppler velocities with a spectrometer could be used. However, up to now, no spatially resolved measurements have been available for motions of flare plasma. Another approach is to extrapolate photospheric fields to the corona and to compare the field lines with loops seen in images. Such comparisons will be useful, even though the existing magnetograms may not have enough spatial or temporal resolution or accuracy for the transverse component, and it is not clear if the flare loops are represented by these extrapolated field lines.

A third approach is purely geometrical, relying on how the loops appear in 2-d images. For studying the 3-d geometry of *non-flaring* coronal loops, stereoscopic techniques have been developed (Berton, Sakurai 1985, Aschwanden et al. 1999). These techniques make use of images at different times, which produce different projections due to solar rotation. However, flare loops are dynamic by nature, and they are by no means stationary. Therefore we have to rely on a single image until simultaneous stereoscopy becomes available in the future. A technique to obtain the loop geometry from a single image was developed and applied to post-flare loops seen in $H\alpha$ images (Loughhead et al. 1983, hereafter LOUGH83). In this report, we first apply the formulation of LOUGH83 to flare data from the Soft X-ray Telescope (SXT) on board *Yohkoh*. It is clear that a single image does not permit us to determine both the loop shape and its inclination with respect to solar surface. We discuss various possible ways of further constraining them.

2. Retrieval of Loop Geometry from a Single Image

Here we make use of the formulation of LOUGH83 (which consists of a multiple trigonometric transformations) to show what we can learn from a single flare image. For simplicity we ignore the finite width of a loop, which is typically more than a few pixels in SXT images (1 SXT pixel = 2.455"). Instead we concentrate on the central loop axis, identifying the loop with a curved line. We further assume that the loop including the footpoints lies in a plane. We take the coordinate of the middle point of the footpoints as the location of the loop on the Sun. These three points are assumed to be on a straight line, implying that the footpoint separation is small enough. Then it is

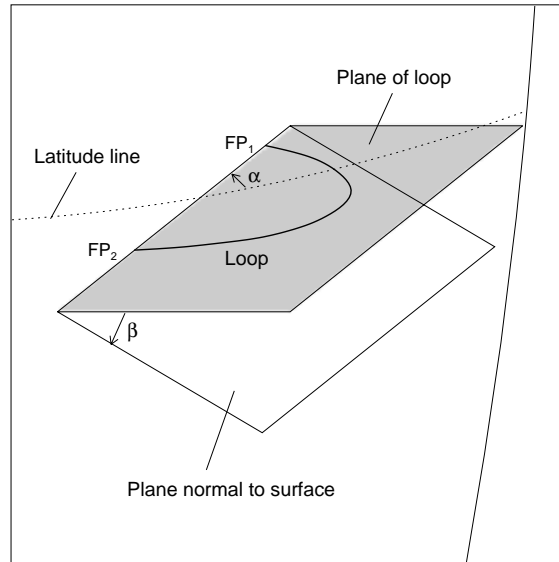


Fig. 1.. Definition of the tilt (α) and inclination (β) of the loop that is contained in the loop plane.

clear that the appearance of the loop at the location is determined by its true shape (viewed face-on), tilt α of the line connecting the footpoints with respect to the latitude line, and inclination β of the loop plane from the plane normal to the surface (see Figure 1).

As illustrated in Figure 2, we mark what seems to be the central axis of the loop. The end points must coincide with the footpoints, which directly give tilt α for the loop location. It is often difficult to see the true footpoints of active region loops in SXT images, primarily because SXT is not sensitive at low ($\lesssim 2.0$ MK) temperatures. Therefore for a more accurate identification, we use the nearly simultaneous image from the Hard X-ray Telescope (HXT). According to Sakao (1994), the double sources often observed in HXT images correspond to footpoints. For the flare loop of Figure 2, we have $\alpha = -61.6^\circ$.

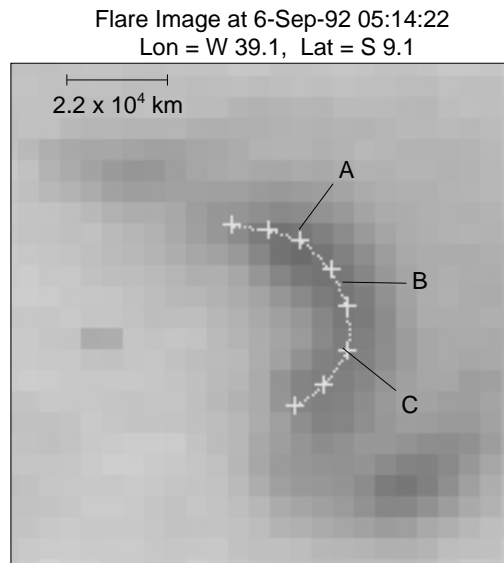


Fig. 2.. SXT flare image. This illustrates marking the central axis of a flare loop. The labels A, B and C are used as fiducial marks for Fig.5

We use equation (7) of LOUGH83 to invert the loop axis in the image plane to the loop plane. In order to do this, we need inclination β , which is unknown. In other words, we have an infinite number of loops that are projected to be the observed loop, because β is arbitrary. Some of them are shown in Figure 3. The only constraint on β a single image provides is its range, in which the loop height becomes positive. For example, β for the observed loop of Figure 2 must be $<31^\circ$.

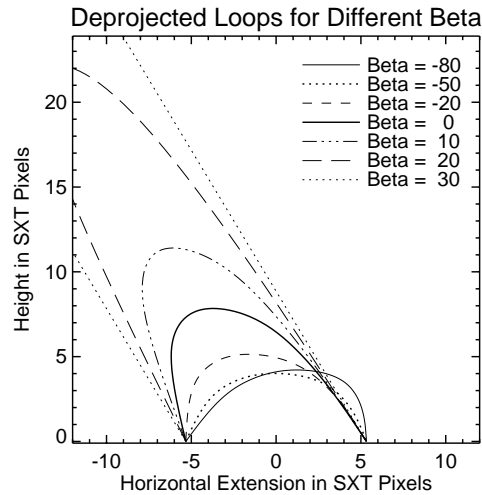


Fig. 3.. Face-on view of the loops for various values of β . The left footpoint corresponds to the southern footpoint in the image plane.

3. Possible Ways of Constraining β

We now have to use other criteria to put a constraint on β or the associated loop shape. One obvious choice is the most symmetric loop, and its derivation was indeed detailed in LOUGH83. In our case, the loops for $-60^\circ < \beta < 50^\circ$ are highly symmetric. However, flare loops may be asymmetric (Kundu, Vlahos 1979, Nitta, Kiplinger, Kai 1989), unlike the $H\alpha$ post-flare loops analyzed in LOUGH83. Another obvious choice would be the loop that stands vertically ($\beta=0^\circ$), as usually assumed when estimating the height of a loop from projection effect. But in this case the loop is far from circular.

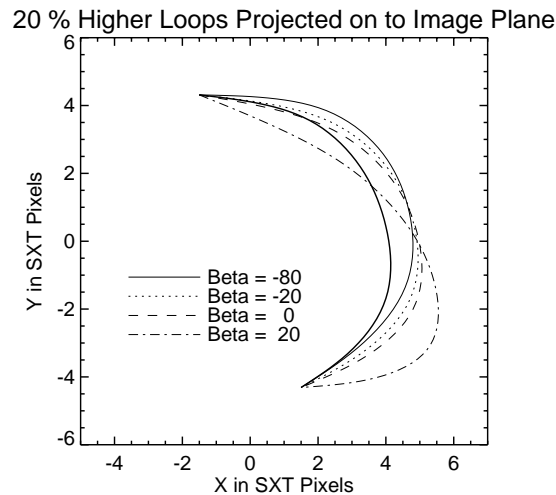


Fig. 4.. Projections into the image plane of the loops of Fig. 3 elongated by 20 % in height. The thick solid line is the observed loop.

The next possibility is to use the evolution of the loop during the flare, which typically takes the form of a rising motion of the loop top in a limb flare. In a disk event, the direction of the apparent motion should depend on how the loop is oriented. Therefore we calculate the projection on to the image plane of the loop elongated in height, hoping that they look different from shorter ones. As far as the flare of Figure 2 is concerned, Figure 4 shows that there is not much difference between the appearances of the elongated loops for $\beta < 0^\circ$. However, the effectiveness of this technique varies with the location and appearance of the flare loop.

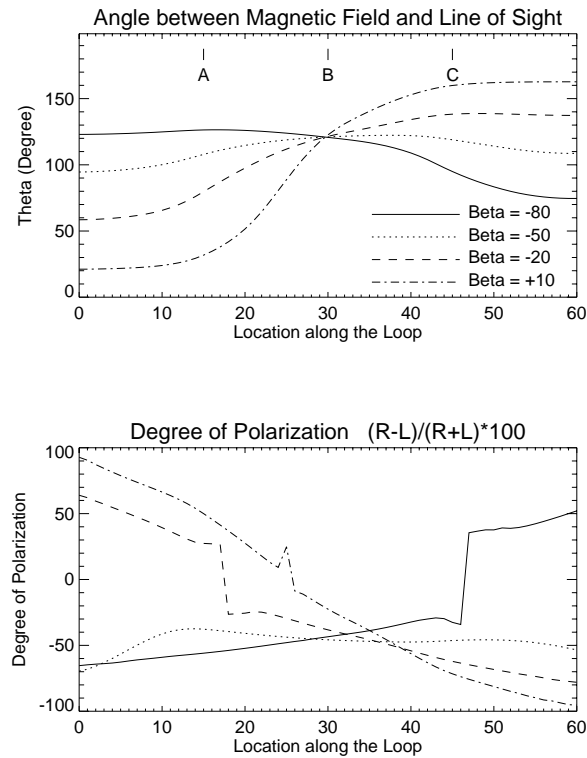


Fig. 5.. Angle of the magnetic field line with the line of sight for two cases of β . The labels A, B and C indicate positions within the loop (see Fig. 2).

Finally, there are observations that are sensitive to the direction of the loop with respect to the line of sight. First, we consider gyrosynchrotron emission from nonthermal electrons as observed in microwaves. These nonthermal electrons are also responsible for hard X-ray and γ -ray emissions, so comparisons of images in these wavelengths and microwaves are expected to give us information on the magnetic field that forms the flare loop. However, the dependence of gyrosynchrotron emission on several unknown parameters generally makes such comparisons less compelling. Here, we concentrate on polarization that appears to be less model dependent. In the upper panel of Figure 5, the angle between the magnetic field and the line of sight is plotted for several values of β , assuming that the northern footpoint has negative polarity. The calculated degree of polarization at 17 GHz is plotted in the lower panel. The overshoot around the polarization reversal (for $\beta=10^\circ$) is a computational artifact. We note that only one polarization occupies the whole loop for $\beta=-50^\circ$. The sense of polarization at the northern part of the loop is opposite between $\beta=-50^\circ$ and $\beta=-20^\circ$. The location of zero polarization is different for different β . The lower panel of Figure 5 results from a particular set of parameters for gyrosynchrotron emission such as

- The high-energy cut-off and power-law index of the electrons are 2 MeV and 4.0, respectively,
- The magnetic field strength has the r^{-3} dependence, where r is the distance from a dipole embedded at the depth of $0.25 \times$ (the footpoint separation).

In reality, the observed polarization may be lower, because of contributions from electrons on different field lines and possible effects of finite optical depth. But note that the general appearance of the lower panel of Figure 5 do

not strongly depend on these parameters. Hard X-ray and γ -ray spectral data and magnetic field extrapolations will improve our understanding of the above parameters.

In addition, even without spatial resolution, spectra of the Bragg Crystal Spectrometer (BCS) may provide another observational test. For example, In the loop for $\beta = 80^\circ$, chromospheric evaporation would be observed as redshift rather than blueshift, because the loop is oriented in such a way that the loop top is farther away than the footpoints. A marginal indication of this phenomenon is actually observed in other flares (Nitta, van Driel-Gesztelyi, Harra-Murnion 1998).

4. Concluding Remarks

We have shown that it is not easy to determine the geometry of flare loops even under the strong assumption that the loop is contained in a plane. But some observations such as the motion of the soft X-ray bright source and polarization in microwaves can be used to constrain the inclination angle β , which determines the intrinsic loop shape.

However, even if we have a reasonable constraint on β , we still do not know if it is appropriate to represent the loop by the central axis or to assume that it is planar. Various observations suggest that loops in flare-productive active regions are twisted. But we will have to postpone sorting out these questions until simultaneous stereoscopy becomes possible by multiple spacecraft.

This work has been supported by NASA grant NAS 8-40801. The author is thankful to H. Hudson for calling his attention to the paper by Loughhead et al.

References

- Aschwanden, M. J. et al. 1999, ApJ, in press
- Berton, R., Sakurai, T. 1985, Sol. Phys., 96, 93
- Kundu, M. R., Vlahos, L. 1979, ApJ, 232, 595
- Loughhead, R. E., Wang, J.-L., Blows, G. 1983, ApJ, 274, 883 (LOUGH83)
- Nitta, N., Kiplinger, A. L., Kai, K. 1989, ApJ, 337, 1003
- Nitta, N., van Driel-Gesztelyi, L., Harra-Murnion, L. K. 1998, Sol. Phys., submitted
- Ogawara, Y. et al. 1991, Sol. Phys., 136, 1
- Sakao, T. 1994, PhD Thesis, University of Tokyo, Tokyo
- Tsuneta, S. 1996, in R. D. Bentley and J. T. Mariska (eds.), Magnetic Reconnection in the Solar Atmosphere, ASP Conference Series, Vol. 111, p. 409